Hindawi
Journal of Food Quality
Volume 2021, Article ID 5356645, 13 pages
https://doi.org/10.1155/2021/5356645

Research Article

Ultrasonic Pretreatment-Assisted Electrohydrodynamic Drying of Potato Slices

Zhiyuan Cao,[1] **Changjiang Ding**,[1,2] **Rui Zhao**,[1] **Zhiqing Song**,[1,2] **and Hao Chen**[1,2]

[1]*College of Science, Inner Mongolia University of Technology, Hohhot 010051, China*
[2]*Inner Mongolia Energy Conservation and Emission Reduction Engineering Technology Research Center for Fermentation Industry, Inner Mongolia University of Technology, Hohhot 010051, China*

Correspondence should be addressed to Changjiang Ding; ding9713@163.com

Received 13 June 2021; Revised 18 September 2021; Accepted 12 October 2021; Published 21 October 2021

Academic Editor: Constantin Apetrei

To investigate the drying characteristics and mechanism during electrohydrodynamic (EHD) drying with ultrasonic pretreatment, the ultrasonic pretreatment-assisted EHD drying method at different power values was used to carry out the drying experiment of potatoes. To carry out this study, potato slices were pretreated with different ultrasonic power values (150, 180, 210, 240, and 270 W) or without ultrasound for 30 min at 30°C. The corresponding voltage was 18 kV during EHD drying. The moisture ratio, drying rate, color, shrinkage, and rehydration rate of potatoes were determined. The microstructure of potatoes was analyzed using infrared spectroscopy and scanning electron microscopy. Eight mathematical models were used to fit the drying of potatoes. Results showed that, compared with the control group, the ultrasonic pretreatment combined with the EHD drying group had improved the drying rate of potato slices, which was different at varying ultrasonic power values. Ultrasonic pretreatment had a remarkable effect on the color of the potato but had little effect on the shrinkage rate. The maximum rehydration rate is 5.7704 at 180 W. The minimum and maximum values of effective moisture diffusivity (D_{eff}) were 3.4070×10^{-7} m^2/s and 4.1160×10^{-7} m^2/s, respectively. The effect of ultrasonic power pretreatment on the microstructure of potato in the EHD drying process was significant ($p > 0.05$). According to the statistical parameter evaluation, eight mathematical models could satisfactorily describe drying curves of potato slices dried under EHD with ultrasonic pretreatment, and the logarithmic model was best suited. This work provides a theoretical basis and practical guidance to further understand the parameter characteristics and mechanism of ultrasonic pretreatment combined with the EHD drying technology.

1. Introduction

Potato, an annual herb of Solanaceae, is the fourth most important food crop in the world after rice, wheat, and corn. At present, more than 150 countries and regions are planting potatoes in the world. As the largest potatoes production and export country in the world, China's potatoes storage and transportation are particularly important. Drying is the most important and common operation in potato processing to extend the shelf life of food products by reducing water activity, introducing new forms of consumption, and minimizing waste. In addition, drying reduces transportation, storage, packaging, and distribution costs by the decrease of product volume and weight [1]. At present, the main drying methods of potatoes are hot-air, vacuum freeze, microwave, and infrared radiation drying methods [2]. Each drying technology has its advantages and disadvantages. Hot-air drying has low cost and high speed. However, the material's active ingredients are lost remarkably, and the quality is poor [2]. The equipment for the vacuum freeze-drying method is expensive [3]. Microwave drying has high heating efficiency, strong processing capacity, and easy operation but results in uneven drying [4]. The infrared radiation drying has an evident thermal effect on the drying process but has no evident enhancement effect on the internal mass transfer [5]. Therefore, new drying technologies should be studied.

Electrohydrodynamic (EHD) drying is a nonthermal food drying technology, which has the advantages of fast drying speed, high drying quality, and energy-saving and is becoming a research hotspot [6–8]. Sriariyakul et al. used EHD drying to dry aloe puree and found that EHD drying can significantly shorten the drying time and increase the drying speed [9]. Martynenko et al. found that EHD drying can increase the drying speed of apples and mushrooms, and the drying rate increases with increasing voltage [10, 11]. Bajgai and Hashinaka observed the low shrinkage rate (SR), high rehydration rate (RR), and good color of Japanese radish after drying under the action of a high-voltage electric field [12]. The ascorbic acid content in spinach after EHD drying is higher than that after oven drying. The EHD drying improves the preservation of sample nutrients [13]. Martynenko and Zheng compared the energy consumption of EHD and low-temperature convective drying methods and found that the energy consumption of EHD drying is only 5.6% of low-temperature convective drying [10]. Esehaghbeygi and Basiry studied the EHD drying of tomato slices and concluded that the energy consumption of oven drying is about 200 times that of EHD drying [14]. However, EHD drying has some disadvantages. For example, when the moisture content of the material is low, the drying speed drops fast, thereby limiting the application of the EHD drying technology in food. This finding also shows that the EHD drying technology still needs improvement in some aspects.

Ultrasonic waves can propagate in gases, liquids, and solids and have the characteristics of good directionality, strong penetrating ability, and strong vibration [15]. When transmitted through a certain medium, ultrasonic waves may cause a rapid vibration in the material and will repeatedly stretch and contract, thereby enhancing the mass transfer effect inside the material after treatment [5]. At present, the application of ultrasonic technology in food drying has attracted attention. Researchers found that the ultrasonic pretreatment of materials can assist other drying technologies to dry materials and improve the drying effect [5]. Bantle and Hanssler dried clipfish using ultrasonic pretreatment combined with convection drying technology and found that the drying time of the ultrasonic treatment group is more than 90% shorter than that of the untreated group at a temperature of 10°C. At 20°C, the drying time of the ultrasonic treatment group is 32.2% shorter than that of the untreated group [16]. Başlar et al. found that the ultrasonic pretreatment combined with the vacuum freeze-drying technology takes about 2.5 times less time to dry chicken and beef meats than the control [17]. Cao et al. found that, compared with the control group, the ultrasonic pretreatment combined with freeze-drying technology group has shortened the drying time of barley grass by 14% and reduced energy consumption by 19% [15]. Xi et al. studied the ultrasonic pretreatment combined with the far-infrared drying of potatoes and found that ultrasonic pretreatment can significantly increase the drying speed and that different drying speeds are obtained with different power values [5]. La Fuente and Tadini studied the ultrasonic pretreatment combined with the hot-air drying of bananas and found that ultrasonic pretreatment can increase the effective diffusion coefficient of moisture in bananas [18]. The ultrasonic pretreatment can be combined with other drying technologies to increase the drying speed of materials. We used the ultrasonic pretreatment combined with the EHD drying to dry wolfberry in the early stage and found that the drying rate of ultrasonic pretreatment of wolfberry is higher than that of the control group and that the ultrasonic pretreatment can overcome some shortcomings of high-voltage electric field drying and improve drying efficiency [19]. The drying process is concerned with the texture and geometry of the materials, as well as the drying technology, and, as such, it is very complex. The same drying technology has different effects on different materials. However, to date, reports about the combined ultrasonic pretreatment and EHD drying of potatoes are not available. Therefore, the aims of this research are to find an efficient nonthermal potato drying method, evaluate the quality of potatoes, model and analyze the drying process, and provide a certain parameter reference for the industrialization process of potato drying.

In this paper, ultrasonic pretreatment combined with EHD drying technology was used to dry potato slices. The drying rate, moisture content, and effective moisture diffusion coefficient of potato slices were measured. The effects of different ultrasonic pretreatment conditions combined with EHD drying on rehydration rate and color of potato slices products were studied. The microstructure changes of potato slices during the drying process were studied by scanning electron microscopy (SEM) and infrared spectroscopy (FTIR). Eight mathematical models were used to fit the drying of potatoes. Single material has undergone a systematic and comprehensive investigation in relation to ultrasonic pretreatment combined with EHD drying processing. It provides an experimental and theoretical basis for the application of ultrasonic pretreatment combined with EHD drying technology in potatoes drying and the exploration of drying mechanisms. At the same time, it provides certain data and theoretical support for the commercialization or industrialization of this new drying method.

2. Materials and Methods

2.1. Experimental Device. The EHD drying experimental device is shown in Figure 1. This device was composed of a high-voltage power supply (YD(JZ)-1.5/50, Wuhan High Voltage Electrical Appliance Factory, Hubei, China), controller (KZX-1.5KVA, Wuhan High Voltage Electrical Appliance Factory, Hubei, China), and a multineedle-to-plate electrode system. The high-voltage power supply could output AC voltage with an adjustable voltage range (0–50 kV). Multineedle electrodes are made of stainless steel. The needle spacing between two needle electrodes was 4 cm, and each needle had a length of 60 mm and a diameter of 1 mm. The needle electrodes were arranged in multiple rows and lined up by stainless steel wire. The ground electrode was a 100 cm × 45 cm stainless steel plate, and a microammeter (C41, Shanghai Precision Instrument Co., Ltd., Shanghai, China) was connected between the bottom plate and the

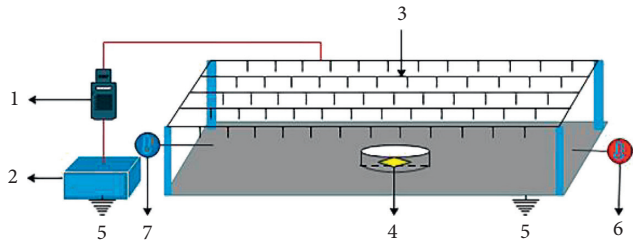

Figure 1: Electrohydrodynamic drying system. 1: high-voltage power source; 2: control system; 3: needle electrode; 4: sample; 5: ground electrode; 6: thermometer; 7: hygrometer.

ground to measure the current generated during the experiment. The distance between the needle tip and the lower electrode plate was 4 cm.

The ultrasonic pretreatment system (KQ-300DE, Kunshan Ultrasonic Instrument Co., Ltd., Jiangsu, China) is shown in Figure 2. This device was composed of an ultrasonic generator, a processing chamber, and a control system. The power range of the ultrasonic generator was 0–300 W, and the water temperature control range was 10°C–80°C. The ultrasonic working frequency was 40 kHz. Since the experiment is still in the laboratory research stage, the maximum capacity of our equipment is small.

After a high voltage is applied to the needle electrode, a very large electric field intensity will be generated near its tip, which will ionize the surrounding air into different types of ions. Under the action of a nonuniform electric field, these charged ions drive other molecules to move together in a directional movement to form an ion wind with a certain speed. When these high-speed moving particles hit the surface of the water-bearing material, they will blow away the water molecules, thereby reducing the nearby moisture, increasing the moisture gradient inside the material, improving the moisture diffusion inside the material, and making it easier for the internal moisture to reach the surface to achieve drying.

2.2. Sample Preparations. Fresh potatoes of regular size and shape were purchased from the supermarket near the Inner Mongolia University of Technology in Hohhot, Inner Mongolia, China, for the experiment. Potatoes were washed and cut into 3 cm × 3 cm × 0.5 cm samples. Potato slices were pretreated with deionized water before the drying experiment to inhibit enzymatic browning effectively during the drying process, placed in the electric heating constant-temperature water tank (DK-600BS, Shanghai Kechen Experimental Equipment Co., Ltd., Shanghai, China) maintained at 100°C for 5 min, collected, and added with deionized water to cool for 5 min. The qualitative filter paper was used to absorb excess water on the surface.

The initial moisture content of potatoes was measured using the rapid moisture tester (Sh10A, Shanghai Precision Instrument Co., Ltd., Shanghai, China), and the initial moisture content was 83% ± 1% (w.b.).

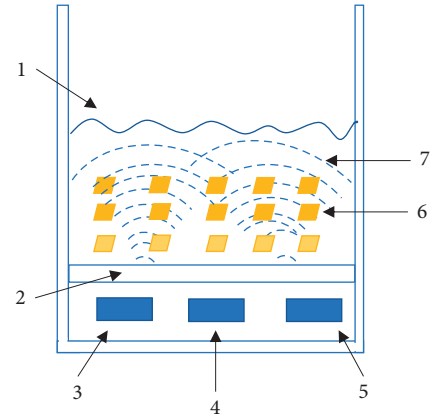

Figure 2: Ultrasonic pretreatment system. 1: deionized water; 2: ultrasonic generator; 3: temperature regulator; 4: time regulator; 5: power regulator; 6: sample; 7: ultrasonic waves.

2.3. Experimental Method. The drying of potatoes was carried out under the conditions of an ambient temperature of 22 ± 1°C, relative humidity of 25% ± 2%, and airflow of 0 m·s^{-1}.

Potato slices treated with deionized water were placed into an ultrasonic processor for pretreatment. The ultrasonic power levels were 0 (Control), 150, 180, 210, 240, and 270 W. The corresponding treatment time was 30 min, and the water temperature was 30°C.

The potato slices pretreated by ultrasound were placed into the EHD drying system for drying experiments. In each run, we place 3 potato slices (4.5 g per piece) inside the chamber. The corresponding voltage was 18 kV during EHD drying.

In the above experiment, the electronic balance (Moilon MTQ200, Sartorius Scientific Instruments (Beijing) Co., Ltd., Beijing, China) was used to record the quality of potato samples every 0.5 h, stop drying until the moisture content is lower than 5% and the moisture content and drying rate of potato samples at different times were calculated in accordance with the formulae (2) and (3). Three samples are processed at a time for each experiment. Each experiment was independently repeated thrice, the number of slices and grams of each repeated experiment is basically the same, and results were expressed as mean ± standard deviation.

2.4. Determination of Moisture Content. The moisture content and ratio of potato slices during drying are defined as follows [3]:

$$M_i = \frac{m_i - m_g}{m_g} \times 100\%, \quad (1)$$

$$\mathrm{MR} = \frac{M_i - M_e}{M_0 - M_e}, \quad (2)$$

where m_g (g) is the dry mass of the potato slice, m_i (g) is the mass of the potato slice after drying for i h, M_0 is the moisture content of the potato slice at time 0, M_i is the

moisture content of the potato slice at time i, M_e is the equilibrium moisture content of potato slices, and MR is the moisture ratio of potato slices.

2.5. Determination of Drying Rate. The drying rate formula of potato slices is as follows [19]:

$$\mathrm{DR} = \frac{M_t - M_{t+\Delta t}}{\Delta t}, \tag{3}$$

where DR (g water per g dry matter·h) is the drying rate, M_t is the moisture content of potato slices at time t, and $M_{t+\Delta t}$ is the moisture content of potato slices at time $t + \Delta t$.

2.6. Determination of Shrinkage Rate. The formula of shrinkage is as follows [1]:

$$\mathrm{SR} = \frac{V_0 - V_f}{V_0} \times 100\%, \tag{4}$$

where SR is the shrinkage of potato slices, V_0 (cm^3) is the volume of fresh potato slices, and V_f (cm^3) is the volume of dry potato slices.

2.7. Determination of Rehydration Rate. Dried potato slices (4.5 g per slice) were added with 100 mL deionized water. The mixture was soaked in the electric heating constant-temperature water tank at 37°C for 7 h. The potato slices were collected, and a qualitative filter paper was used to remove the excess water on the surface. The quality of potato chips before and after rehydration was recorded and determined using the electronic balance. The RR of potato slices was calculated using the following equation [19]:

$$\mathrm{RR} = \frac{m_a}{m_b}, \tag{5}$$

where RR is the rehydration rate of potato slices, m_a (g) is the mass of potato slices after rehydration, and m_b (g) is the mass of potato slices before rehydration.

2.8. Determination of Sample Color Difference. The brightness (L^*), redness (a^*), and yellowness (b^*) values of fresh and dried potato slices were measured using the automatic colorimeter (3nh-NR60CP, Shenzhen Sanenshi Technology Co., Ltd., Shenzhen, China). For the same sample, the experiment was repeated five times, and the average value was taken as the experimental result [10].

$$\Delta E = \sqrt{\left(L^*_1 - L^*_0\right)^2 + \left(a^*_1 - a^*_0\right)^2 + \left(b^*_1 - b^*_0\right)^2}, \tag{6}$$

where L^*_0, a^*_0, and b^*_0 are the brightness, redness, and yellowness values, respectively, of the potato sample before drying. L^*_1, a^*_1, and b^*_1 are the brightness, redness, and yellowness values, respectively, of potato slices after drying.

2.9. Determination of the Effective Moisture Diffusion Coefficient (D_{eff}). D_{eff} during drying was calculated using Fick's second law and expressed as [20]

$$\frac{\mathrm{d}M}{\mathrm{d}t} = D_{\mathrm{eff}} \frac{\mathrm{d}^2 M}{\mathrm{d}r^2}. \tag{7}$$

For long drying processes, MR < 0.6, and the equation can be expressed as follows [11]:

$$\mathrm{MR} = \frac{8}{\pi^2} \cdot \exp\left(-\frac{\pi^2 D_{\mathrm{eff}} t}{4L^2}\right), \tag{8}$$

where D_{eff} is the effective moisture diffusion coefficient of the sample and L is half of the thickness of the sample. The above equation can be written as [11]

$$\ln(\mathrm{MR}) = -\frac{\pi^2 D_{\mathrm{eff}}}{4L^2} t + \ln\left(\frac{8}{\pi^2}\right). \tag{9}$$

D_{eff} can be measured from the relationship between ln (MR) and time. The D_{eff} under each ultrasonic power was calculated by substituting the experimental data in the above formula. This coefficient was determined by simulating the relationship between experimental data ln (MR) and drying time. According to formula (9), the drying time graph gives a straight line with a slope, which can be expressed as [20]

$$\mathrm{slope} = -\frac{\pi^2 D_{\mathrm{eff}}}{4L^2}. \tag{10}$$

Formula (10) is based on the assumption that the moisture diffusion coefficient is constant under the effect of each ultrasonic power and used to obtain the linear change in ln (MR) with drying time.

2.10. Determination of the Infrared Spectrum. Dried potato products were crushed, ground, mixed with potassium bromide at a ratio of 1 : 50, sieved, and placed in the hy-12 tablet press. The sample was scanned in the Fourier transform infrared spectrometer (IRTracer-100, SHIMADZU, Kyoto, Japan) to remove the interference of background, and the infrared scanning spectrum of the sample was obtained.

2.11. Scanning Electron Microscopy (SEM). Dried potato slices were sprayed with gold and placed into the thermal field-emission SEM (Gemini300, Guangzhou Xingzhen Technology Co., Ltd., Guangzhou, China). The scale and magnification of 200 μm and 50 were selected to observe the microstructure of potato samples and the effects and changes in the surface microstructure of each treatment group.

2.12. Determination of the Protein Secondary Structure. The amide I band in the infrared spectrum was used to assign a secondary structure to protein. In accordance with the theoretical calculation of infrared spectroscopy data, the percentages of α-helix, β-sheet, β-turn, β-antiparallel, and random coil to the secondary structure of the protein were determined.

2.13. Mathematical Model Fitting and Parameter Statistics. Table 1 shows eight mathematical models. The semiempirical and empirical mathematical models of thin-layer

Table 1: Mathematical models.

Model	Model equation	References
Lewis	$MR = e^{-at}$	[21]
Page	$MR = e^{-at^b}$	[20]
Silva et al.	$MR = e^{-at-b\sqrt{t}}$	[22]
Wang & Singh	$MR = at^2 + bt + 1$	[23]
Weibull	$MR = e^{((-t/a)^b)}$	[22]
Handerson & Pabis	$MR = ae^{-bt}$	[23]
Logarithmic	$MR = a + be^{-ct}$	[20]
Parabolic	$MR = a + bt + ct^2$	[21]

drying were used to fit the experimental data. The chi-squared (χ^2), R-squared (R^2), and root mean square error (E_{RMS}) values were used to determine the quality of the fit. E_{RMS} gives the deviation between predicted and experimental values. A high R^2 (maximum value of 1) results in low χ^2, which means that the mathematical model is suitable for simulating the drying process of materials. A simulation diagram of predicted and experimental MRs was drawn.

The parameter calculation formula is as follows [17]:

$$R^2 = 1 - \frac{\sum_{i=1}^{N}\left(MR_{exp,i} - MR_{pre,i}\right)^2}{\sum_{i=1}^{N}\left(MR_{exp,i} - \overline{MR}_{exp}\right)^2}, \quad (11)$$

$$\chi^2 = \frac{\sum_{i=1}^{N}\left(MR_{exp,i} - MR_{pre,i}\right)^2}{N - n}, \quad (12)$$

$$E_{RMS} = \sqrt{\frac{1}{N}\sum_{i=1}^{N}\left(MR_{pre,i} - MR_{exp,i}\right)^2}, \quad (13)$$

where $MR_{exp,i}$ is the experimental MR found in any measurement, $MR_{pre,i}$ is the predicted MR for this measurement, $\overline{MR}_{exp}$ is the total average data, N is the number of experimental measurements, and n is the number of constants in the drying model.

2.14. Statistical Analysis. A factorial experiment with a randomized complete design was used to analyze the effect of ultrasound pretreatment at 6 levels (Control, 150, 180, 210, 240, and 270 W) each with three replications (18 treatments). One-way ANOVA and significance analysis were performed using relevant data analysis software. The differences in drying rate, moisture content, RR, shrinkage, and color of potato slices were determined using one-way ANOVA. $p < 0.05$ indicated a significant difference. The Pearson test was used to analyze the correlation between parameters.

3. Results and Discussion

3.1. Effect of Different Ultrasonic Power Pretreatment Conditions on the MR of Potato Slices. Figure 3 shows the effect of different ultrasonic power pretreatment conditions on the change in MR during the EHD drying process. In Figure 3, the use of 180 W ultrasonic pretreatment resulted in the fastest decrease in moisture content. The drying speed

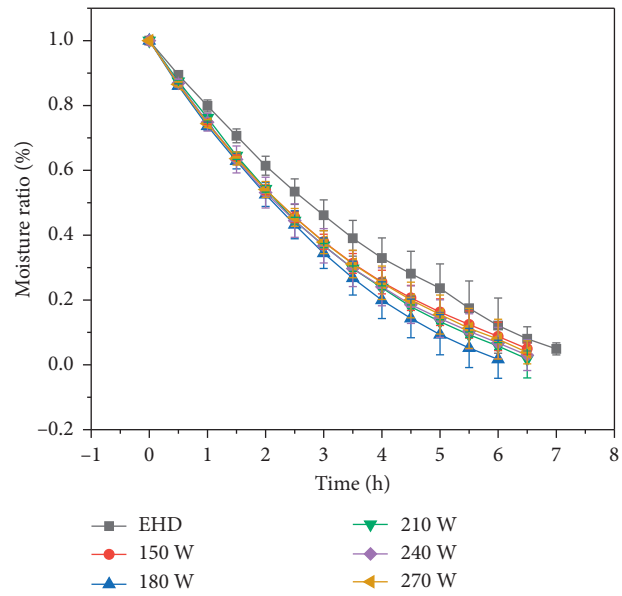

Figure 3: Diagram of the moisture ratio change in potato slices under different ultrasonic pretreatment conditions.

followed the order: 180 W > 210 W > 240 W > 270 W > 150 W > control. After ultrasonic pretreatment, the moisture content of potatoes decreased significantly faster than the control. Jarahizadeh and Taghian Dinani used ultrasonic pretreatment combined with convection to dry potatoes and concluded that the rates of decrease in the moisture content of the ultrasonic pretreatment groups are significantly higher than those of the control group [24]. The results of ultrasonic pretreatment combined with infrared freeze-dried sweet potato slices show that the moisture content of sweet potato after ultrasonic pretreatment decreases faster than that of the control [25]. These findings were consistent with our experimental results.

3.2. Effect of Different Ultrasonic Power Pretreatment Conditions on the Drying Rate of Potato Slices. Figure 4 shows the effect of different ultrasonic power pretreatment conditions on the change in drying ratio during the EHD drying process. Figure 4 shows that, in the initial stage, the drying rate was high and gradually decreased as moisture content decreased. The drying rate of ultrasonic pretreatment was higher than that of the control group, and varying changes in ultrasonic power also changed the drying rate of potato slices. The drying speed followed the order: 180 W > 210 W > 240 W > 270 W > 150 W > control. The drying rate of potato slices with ultrasonic pretreatment combined with EHD drying increased first and then decreased, and the drying rate of the pretreatment group was significantly higher than that of the control group. Puig et al. used ultrasonic pretreatment combined with the convection drying of eggplant and obtained that the drying rate of the ultrasonic pretreatment group was significantly higher than that of the control group [26]. Figure 5 shows that the average drying rate of the sample after ultrasonic pretreatment is significantly ($p < 0.05$) improved compared to the control

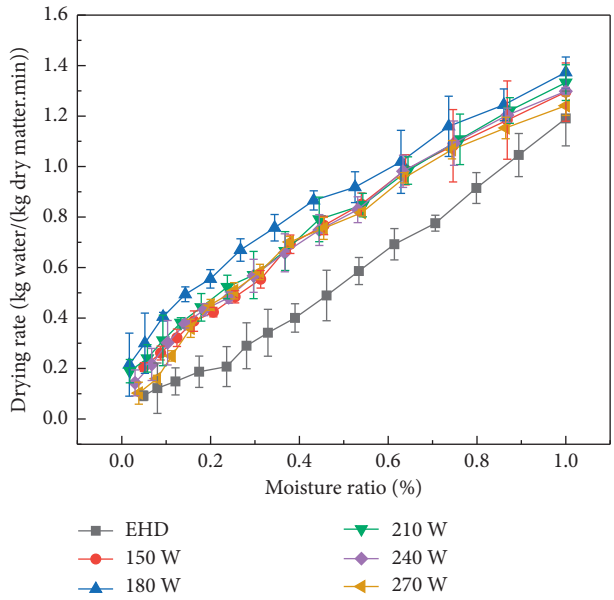

Figure 4: Diagram of the drying rate change in potato slices under different ultrasonic pretreatment conditions.

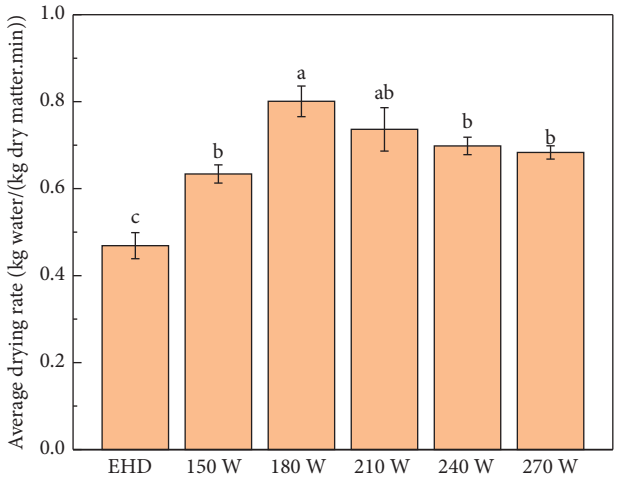

Figure 5: Diagram of the average drying rate change in potato slices under different ultrasonic pretreatment conditions. Data are shown as the mean ± SD. For each response, means with different lowercase letters are significantly different ($p < 0.05$).

group. Under the condition of 180 W, the average drying rate reaches the maximum value. Xi et al. studied the ultrasonic power combined with far-infrared radiation to dry potato slices and found that, compared with the control, the ultrasonic pretreatment could increase the average drying rate of the material. [5]. This finding was the same as our experimental results, which further confirmed that the ultrasonic pretreatment had a positive effect on improving the drying rate.

3.3. Effect of Different Ultrasonic Power Pretreatment Conditions on the RR of Potato Slices. The rehydration characteristics of dried products can well reflect the physicochemical changes in samples during the drying process and can be used as an index to evaluate the quality of dried samples. Figure 6 shows the effect of different ultrasonic power pretreatment conditions on the change in RR during the EHD drying process. The RR followed the order: 180 W > 210 W > 240 W > 150 W > 270 W > control. The RRs were 5.7704, 4.8367, 4.2537, 3.7579, 3.4977, and 2.8336, respectively. The appropriate ultrasonic power could increase the RR of potato slices. When the ultrasonic wave exceeded a certain power, the RR of potato slices decreased to a certain extent. However, a high power did not necessarily mean improved quality. Duan et al. studied the ultrasonic pretreatment combined with the microwave freeze-drying of sea cucumbers and found that, compared with the osmotic solution pretreatment combined with microwave freeze-drying and direct microwave freeze-drying without pretreatment, the rehydration ability of dried products improved evidently after ultrasonic pretreatment [27]. The ultrasonic pretreatment can improve the rehydration ability of dry products due to the damage of the cell wall caused by ultrasonic waves, resulting in serious surface tissue collapse, enhanced water penetration into the cell, and improved RR [28]. Previous studies showed that ultrasonic pretreatment combined with high-voltage electric field drying can significantly improve the RR of dried wolfberry products [19], and this finding was consistent with our experimental results.

3.4. Effect of Different Ultrasonic Power Pretreatment Conditions on the SR of Potato Slices. Figure 7 shows the effect of different ultrasonic power pretreatment conditions on the change in the SR during the EHD drying process. The SRs of potato slices subjected to ultrasonic power values of 0 (control), 150, 180, 210, 240, and 270 W were 0.8158, 0.8217, 0.8664, 0.8383, 0.8516, and 0.8407, respectively (Figure 7). The one-way ANOVA showed no significant difference among treatment groups ($p > 0.05$). Shrinkage is an important parameter to evaluate the quality of materials after drying. Shrinkage is remarkably correlated with the structural characteristics and final moisture content of materials but has a small correlation with the drying method. Bai et al. dried scallop muscle by using the EHD drying and found that the final shrinkage values of the EHD drying (63.70%) and control (65.81%) groups were not significantly ($p > 0.05$) different [29]. Esehaghbeygi et al. found no significant difference in the shrinkage of banana slices after drying at electric field intensities of 6, 8, and 10 kV·cm^{-1} [30]. The EHD drying of wolfberry in the early stage was studied, and results showed that the SRs of wolfberry after drying at 0, 20, 24, 28, and 32 kV were 73.581%, 73.665%, 73.624%, 71.834%, and 72.760%, respectively, and had no significant difference [31]. These studies were consistent with our experimental results.

3.5. Effect of Different Ultrasonic Power Pretreatment Conditions on the Color of Potato Slices. Color is an important parameter of food quality. In the drying process of dehydrated vegetables, compounds in the material in the form of

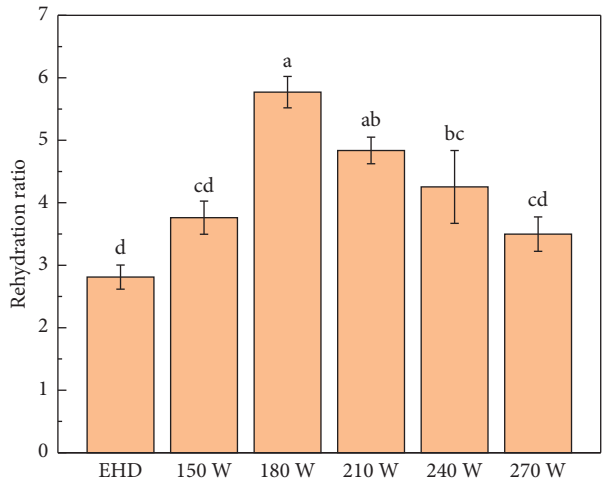

Figure 6: Diagram of the rehydration rate change in potato slices under different ultrasonic pretreatment conditions. Data are shown as the mean ± SD. For each response, means with different lowercase letters are significantly different ($p < 0.05$).

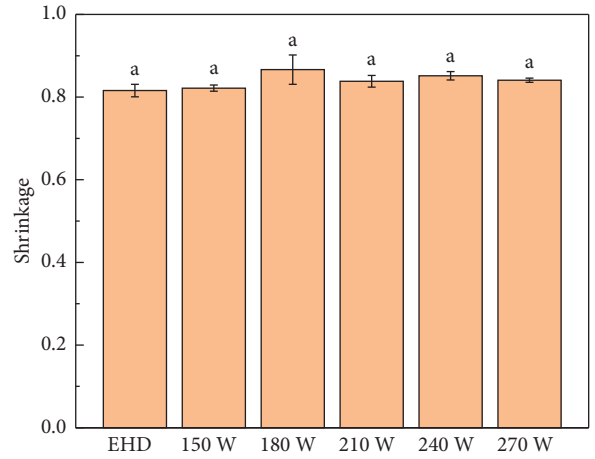

Figure 7: Diagram of the shrinkage rate change in potato slices under different ultrasonic pretreatment conditions. Data are shown as the mean ± SD. For each response, means with different lowercase letters are significantly different ($p < 0.05$).

polyphenols may affect the color and flavor of the treated tissue due to Maillard reaction, pigment degradation, enzymatic browning, vitamin C oxidation, and other factors [30]. Table 2 shows the color difference changes in potato slices before and after drying under different ultrasonic power pretreatment conditions. Table 2 shows that the L^* values of dried potato slices are significantly different from those of fresh potato slices ($p > 0.05$). However, little differences between a^* and b^* values were observed. L^* of the potato after ultrasonic pretreatment was significantly lower than that of the control, and no significant difference among the pretreatment groups was observed ($p > 0.05$), which might be due to the strong inhibitory effect of ultrasonic pretreatment on the activity of polyphenol oxidase. The a^* values of potatoes after ultrasonic pretreatments except those treated at 240 W were higher than those of the control ($p > 0.05$). The change in a^* was due to the Maillard reaction during drying. The values of b^* in all treatment groups were lower than those in the control group (32.6813). Wu et al. used ultrasound to pretreat sweet potatoes and found that as the ultrasound power increases, L^* and b^* decrease. These findings were similar to our experimental results [23]. ΔE was calculated to determine the color change. As the power increased, ΔE first increased and then decreased, reaching a minimum value (9.8281) at 240 W.

3.6. Effect of Different Ultrasonic Power Pretreatment Conditions on D_{eff} of Potato Slices. Table 3 shows that, under ultrasonic pretreatment, D_{eff} of potato slices could be improved. With increasing power, D_{eff} first increased and then decreased. In the 180 W ultrasonic pretreatment group, D_{eff} reached the highest value (4.1660×10^{-7} m^2·s^{-1}). Appropriate ultrasonic power pretreatment could maximize the ability of effective moisture diffusion and then improve the drying efficiency of potato slices. Zhao et al. used ultrasonic pretreatment combined with microwave vacuum to dry lotus seeds and found that ultrasonic treatment at 20 or 35 kHz significantly accelerated the drying speed and increased D_{eff}. At ultrasonic treatment of 80 kHz, no increase in drying rate was observed [32]. This finding also explained that not all ultrasonic pretreatment power could increase the D_{eff} in the material and improved the drying speed, which was the same as our experimental results. When the ultrasonic power increased to a certain extent, the cavitation effect was limited, and D_{eff} decreased.

3.7. Effect of Different Ultrasonic Power Pretreatment Conditions on the Infrared Spectrum of Potato Slices. Figure 8 shows the infrared spectra of potato pretreated with different ultrasonic power values. The infrared spectra of potato slices under different ultrasonic power pretreatment conditions were similar, and the positions of spectral bands were relatively close (Figure 8). However, the characteristic absorption peak intensities were significantly different. The absorbance increased first and then decreased with increasing power. The spectral peak positions were similar. Compared with those of the control group, the characteristic band intensities of 150, 180, and 210 W pretreatment groups were larger, and those of 240 and 270 W pretreatment groups were smaller. At different ultrasonic power pretreatment conditions, the chemical components of potatoes were the same, but the appropriate ultrasonic power pretreatment could remarkably preserve effective nutrients. Data showed that the main characteristic absorption peaks in the infrared spectrum were assigned. The stretching vibrations of N-H and O-H of polysaccharides, glycosides, amino acids, and proteins were observed near 3408 cm^{-1} [33]. The C-H stretching vibration of fatty acids was near 2937 cm^{-1} [33]. The C=O stretching vibration of carboxylic acids or esters was near 1650–1630 cm^{-1} [34]. The peak near 1417 cm^{-1} was attributed to fructose, and the peak near 1155 cm^{-1} was the C-O stretching vibration of fructose. The peak near 1034 cm^{-1} was the C-O stretching vibration of glucose, C-C stretching vibration, and C-O-H bending

Table 2: Color difference changes in potatoes before and after drying under different ultrasonic power pretreatment conditions.

Power	L^*	a^*	b^*	ΔE^*
Fresh	65.8810 ± 1.1350^{a}	3.3047 ± 0.2365^{bc}	29.6543 ± 1.8291^{ab}	—
Control	$49.5650 \pm 2.0537^{b}\downarrow$	$3.3260 \pm 0.2266^{b}\uparrow$	$32.6813 \pm 1.1714^{a}\uparrow$	10.7697 ± 0.5095^{b}
150 W	$42.2677 \pm 0.2990^{c}\downarrow$	$4.8923 \pm 0.1857^{ab}\uparrow$	$28.7000 \pm 0.3376^{b}\downarrow$	$13.9246 \pm 0.5920^{a}\uparrow$
180 W	$41.6267 \pm 0.9689^{c}\downarrow$	$4.0117 \pm 0.2729^{b}\uparrow$	$25.3710 \pm 0.4482^{bc}\downarrow$	$11.7631 \pm 0.8309^{b}\uparrow$
210 W	$41.5807 \pm 0.7307^{c}\downarrow$	$5.3187 \pm 0.3991^{a}\uparrow$	$29.4643 \pm 0.4117^{ab}\downarrow$	$10.9377 \pm 0.7059^{b}\downarrow$
240 W	$43.6750 \pm 0.5110^{c}\downarrow$	$2.3957 \pm 0.3649^{c}\downarrow$	$24.8277 \pm 0.5895^{c}\downarrow$	$9.8281 \pm 0.6680^{b}\downarrow$
270 W	$40.6087 \pm 0.1839^{c}\downarrow$	$3.5007 \pm 0.0756^{b}\uparrow$	$25.1860 \pm 1.6045^{bc}\downarrow$	$10.5204 \pm 1.4174^{b}\downarrow$

Table 3: Effect of different ultrasonic power pretreatment conditions on the effective moisture diffusion coefficient of potato slices.

Power	Linear analog equation	R^2	$D_{\text{eff}} \times 10^{-7}$ (m^2/s)
Control	$\ln(MR) = -0.1345t + 0.9155$	0.9778	3.4070
150 W	$\ln(MR) = -0.1416t + 0.8764$	0.9545	3.5870
180 W	$\ln(MR) = -0.1625t + 0.8952$	0.9670	4.1160
210 W	$\ln(MR) = -0.1488t + 0.8873$	0.9593	3.7690
240 W	$\ln(MR) = -0.1454t + 0.8769$	0.9548	3.6830
270 W	$\ln(MR) = -0.1432t + 0.8773$	0.9577	3.6270

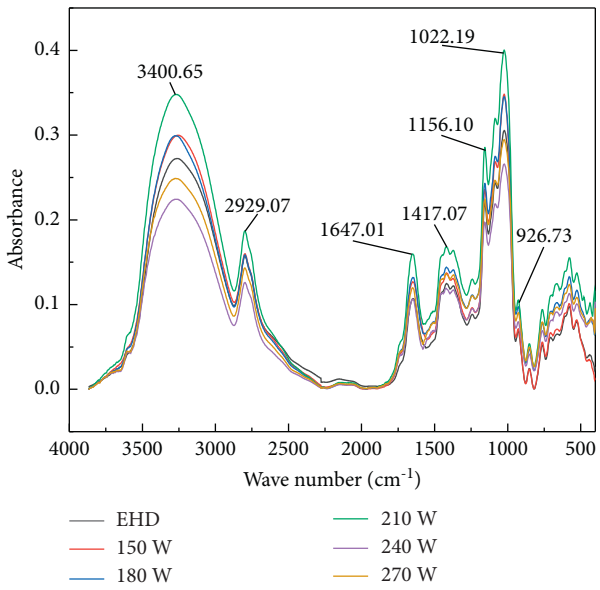

Figure 8: Infrared spectra of potato slices under different ultrasonic pretreatment conditions.

vibration, and the peak near 929 cm^{-1} was the C-C stretching vibration [35]. Figure 8 shows the effect of different ultrasonic power pretreatment conditions on the effective nutrients of potato slices subjected to EHD drying and provides a deep understanding of the EHD drying mechanism combined with ultrasonic power pretreatment.

3.8. Effect of Different Ultrasonic Power Pretreatment Conditions on the Surface Microstructures of Potato Slices. Figure 9 shows the surface microstructure of potato slices pretreated with different ultrasonic power values. Figure 9 shows that the control group had deep textures and no evident pore. Textures became shallow after ultrasonic pretreatment and smoothened as the power increased. Some pores were observed in the 150, 180, 210, and 240 W ultrasonic pretreatment groups. The cavitation effect of ultrasonic waves destroyed the surface texture of the material and smoothened the texture. Some pores were created under a certain power, thereby accelerating the water loss of the material and increasing the drying rate. Rashid et al. studied the ultrasonic pretreatment of potatoes and found pores [36]. As the power increased to 270 W, the surface of potato slices smoothened. Puig et al. subjected eggplant to ultrasonic pretreatment and showed similar results [26]. Garcia-Perez et al. studied the ultrasonic drying of orange peels and found that, with increased ultrasonic power, the pores produced by the cavitation effect increased first and then decreased [37]. This finding was similar to our experimental results. The microstructure analysis further confirmed that the ultrasonic pretreatment had a remarkable influence on the surface of potatoes and affected the drying speed, quality, and various indicators of potato slices.

3.9. Effect of Different Ultrasonic Power Pretreatment Conditions on the Protein Secondary Structure of Potato Slices. Table 4 shows the calculation results of the protein secondary structure. The shape of the amide I band ranging from 1600 cm^{-1} to 1700 cm^{-1} was used to determine the secondary structure of the protein [38]. The corresponding relationship between each subpeak and secondary structure was as follows: 1610–1642 cm^{-1}, β-sheet; 1642–1650 cm^{-1}, random coil; 1650–1660 cm^{-1}, α-helix; 1660–1680 cm^{-1}, β-turn; and 1680–1700 cm^{-1}, β-antiparallel [39]. α-helix and β-sheet (parallel and antiparallel) represented ordered structures, whereas β-turn and random coils represented disordered structures [40]. Table 4 shows that the content of the random coil increased with increasing power. The content of α-helix in the pretreatment group was lower than that in the control group. The content of β-turn in the pretreatment group was higher than that in the control group. The content of β-antiparallel remained unchanged, and the content of β-sheets gradually decreased with

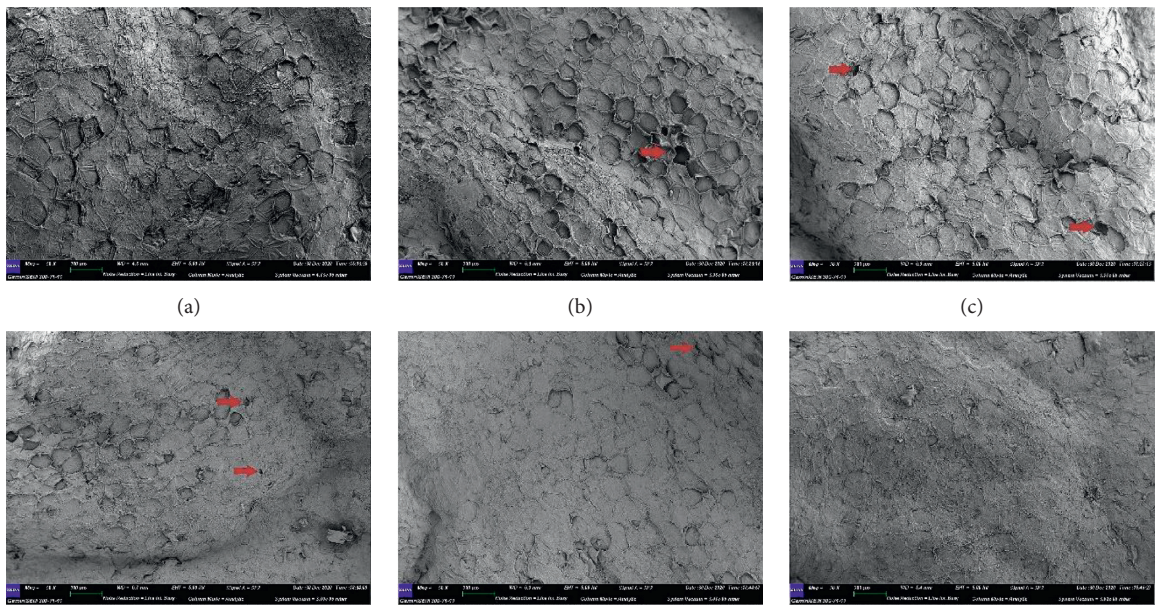

(a) (b) (c)

(d) (e) (f)

Figure 9: Microstructures of potato slices pretreated with different ultrasonic power values: (a) 0 (control), (b) 150, (c) 180, (d) 210, (e) 240, and (f) 270 W.

Table 4: Calculation results of protein secondary structure.

Conditions	Random coil (%)	α-Helix (%)	β-Turn (%)	β-Antiparallel (%)	β-Sheet (%)
Control	7.83	19.35	25.54	7.92	37.73
150 W	11.29	12.09	30.04	6.30	38.38
180 W	11.58	11.56	27.48	9.85	39.54
210 W	13.82	14.26	33.76	5.35	32.80
240 W	14.21	7.28	33.14	6.93	31.15
270 W	23.33	11.56	26.78	8.23	30.10

increasing power. These experimental results provided a new idea for the research of ultrasonic pretreatment and EHD drying mechanisms.

3.10. Statistical Analysis Results of MR and Drying Time Modeling. Table 5 shows the fitting results of the drying mathematical model. Eight thin-layer drying models were fitted with the experimental data by using software, and the goodness-of-fit indices, such as R^2, χ^2, and E_{RMS}, were used to evaluate the fitted drying models. Results are shown in Table 5. The R^2 values of eight models were greater than 0.95 (Table 5), indicating that the eight thin-layer drying mathematical models could be used to simulate the drying process of potato slices with different ultrasonic power values. Among them, the logarithmic thin-layer drying mathematical model showed that R^2 was 0.99950–1.00000, which was the maximum value of eight thin-layer drying mathematical models and closest to 1. χ^2 was 0.000002–0.000056, and E_{RMS} of 0.001366–0.007503 was the minimum value of eight thin-layer drying mathematical models. Therefore, the logarithmic thin-layer drying mathematical model was the most suitable to simulate the drying process of potato slices with different ultrasonic power values. Figure 10 shows the comparison between predicted and experimental MRs. The slope of the graph drawn using the logarithmic model prediction and the experimental moisture content data (Figure 10) was approximately 1, which further proved that the logarithmic model was suitable for the fitting of the drying curve of potato slices subjected to combined EHD drying and ultrasonic pretreatment.

3.11. Analysis of Correlation Coefficient Results. Figure 11 shows the Pearson correlation coefficient of potato slices pretreated at different ultrasonic power values. The root cause between the internal and external changes was explored through the calculation and analysis of the Pearson correlation coefficient. T had a significant and negative correlation with β-sheet ($r = -0.87$) and a significant and positive correlation with the random coil ($r = 0.90$). MR was significantly and negatively correlated with RR ($r = -0.97$) and SR ($r = -0.91$). DR was significantly and negatively correlated with L^* ($r = -0.92$). RR was significantly and positively correlated with SR ($r = 0.84$). b^* was significantly positively and correlated with α-helix ($r = 0.91$).

Table 5: Statistical analysis results of moisture ratio and drying time modeling.

Model	Conditions	a	b	c	R^2	χ^2	E_{RMS}
Lewis	Control	0.2730	—	—	0.98496	0.001205	0.034710
	150 W	0.3329	—	—	0.99211	0.000690	0.026260
	180 W	0.3756	—	—	0.97494	0.002594	0.050930
	210 W	0.3461	—	—	0.98275	0.001656	0.040700
	240 W	0.3461	—	—	0.98830	0.001081	0.032880
	270 W	0.3367	—	—	0.99036	0.000857	0.029270
Page	Control	0.2096	1.2170	—	0.99685	0.000227	0.015080
	150 W	0.2788	1.1570	—	0.99890	0.000106	0.010280
	180 W	0.2700	1.3050	—	0.99460	0.000606	0.024620
	210 W	0.2603	1.2560	—	0.99820	0.000193	0.013890
	240 W	0.2772	1.2000	—	0.99850	0.000154	0.012420
	270 W	0.2779	1.1700	—	0.99810	0.000182	0.013500
Silva et al.	Control	0.3519	−0.1392	—	0.99460	0.000471	0.021710
	150 W	0.4061	−0.1233	—	0.99750	0.000240	0.015490
	180 W	0.5151	−0.2284	—	0.98890	0.001259	0.035480
	210 W	0.4643	−0.1969	—	0.99490	0.000538	0.023200
	240 W	0.4411	−0.1582	—	0.99630	0.000370	0.019230
	270 W	0.4142	−0.1303	—	0.99620	0.000366	0.019130
Wang & Singh	Control	0.0115	−0.2133	—	0.99940	0.000050	0.007068
	150 W	0.0191	−0.2641	—	0.99940	0.000055	0.007434
	180 W	0.0185	−0.2743	—	0.99990	0.000013	0.003566
	210 W	0.0179	−0.2633	—	0.99980	0.000019	0.004387
	240 W	0.0191	−0.2684	—	0.99960	0.000037	0.006102
	270 W	0.0187	−0.2638	—	0.99930	0.000063	0.007961
Weibull	EHD	3.6110	1.2170	—	0.99740	0.000227	0.015080
	150 W	3.0160	1.1570	—	0.99890	0.000106	0.010280
	180 W	2.7270	1.3050	—	0.99460	0.000606	0.024620
	210 W	2.9210	1.2560	—	0.99820	0.000193	0.013890
	240 W	2.9140	1.2000	—	0.99850	0.000154	0.012420
	270 W	2.9870	1.1700	—	0.99810	0.000182	0.013500
Handerson & Pabis	Control	1.0410	0.2867	—	0.98860	0.000994	0.031520
	150 W	1.0320	0.3448	—	0.99400	0.000571	0.023890
	180 W	1.0540	0.3963	—	0.97940	0.002331	0.048280
	210 W	1.0510	0.3649	—	0.98700	0.001361	0.036890
	240 W	1.0410	0.3613	—	0.99110	0.000895	0.029920
	270 W	1.0330	0.3490	—	0.99240	0.000741	0.027230
Logarithmic	Control	−0.4260	1.4290	0.15780	0.99960	0.000038	0.006165
	150 W	−0.1788	1.1830	0.24900	0.99990	0.000008	0.002759
	180 W	−0.3529	1.3570	0.22100	0.99970	0.000038	0.006194
	210 W	−0.2788	1.2900	0.22760	0.99950	0.000056	0.007503
	240 W	−0.2161	1.2230	0.24550	0.99980	0.000019	0.004340
	270 W	−0.2099	1.2110	0.24010	1.00000	0.000002	0.001366
Parabolic	Control	0.9974	−0.2116	0.01126	0.99944	0.000054	0.007324
	150 W	0.9916	−0.2588	0.01834	0.99950	0.000047	0.006874
	180 W	0.9946	−0.2709	0.01807	0.99990	0.000008	0.002894
	210 W	1.0010	−0.2640	0.01795	0.99980	0.000021	0.004573
	240 W	0.9948	−0.2651	0.01869	0.99970	0.000036	0.005969
	270 W	0.9894	−0.2570	0.01781	0.99960	0.000048	0.006915

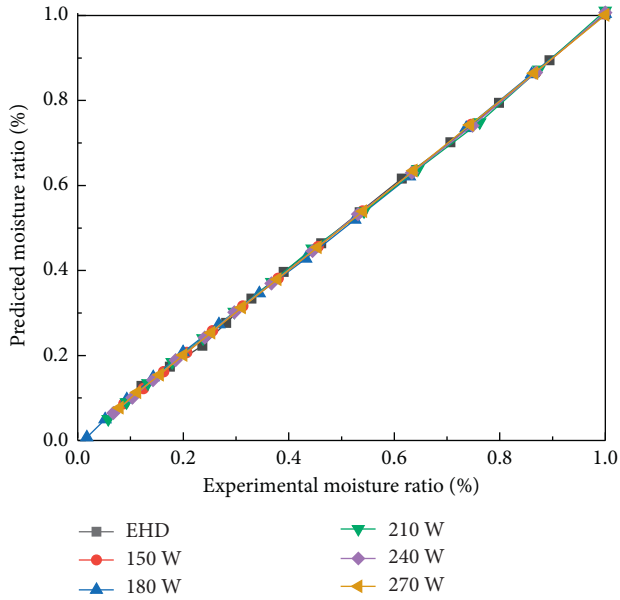

Figure 10: Moisture ratio predicted by the logarithmic model and the experimental moisture ratio.

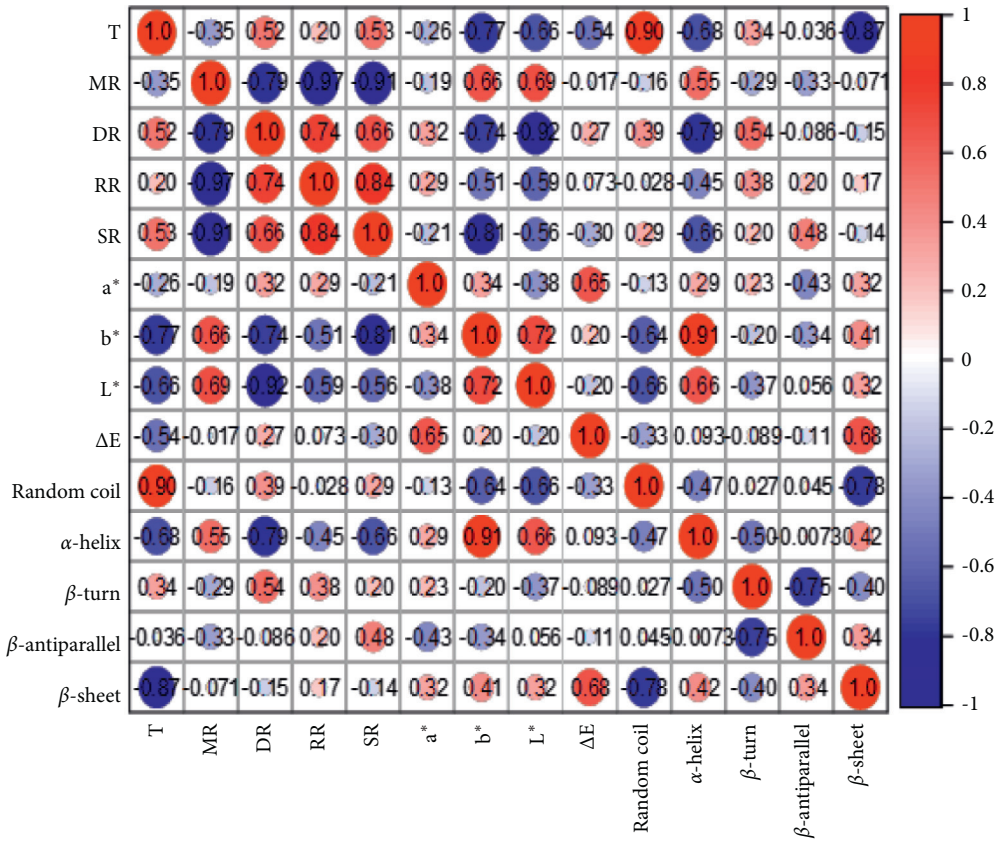

Figure 11: Pearson's correlation coefficient matrix. *T*, drying time; RR, rehydration rate; SR, shrinkage rate.

4. Conclusion

Different ultrasonic power pretreatments were combined with a high-voltage electric field to dry potato slices. The ultrasonic power was best maintained between 180 and 210 W. After ultrasonic pretreatment, the drying rate of potato slices was significantly increased, which shortened the drying time and preserved effective nutrients. Compared with the control group, pretreatment groups had increased RR, but the SR did not change significantly. The infrared

spectrum showed that the peak intensity of each functional group in the ultrasonic pretreatment group was significantly different from that in the control group. SEM was used to observe the surface of potato slices and showed that the ultrasonic pretreatment could significantly change the surface microstructure of potato slices. A high ultrasonic power resulted in a significant effect. Calculating the secondary structure of protein showed that the ultrasonic pretreatment with different power values could change the contents of β-sheet, random coil, α-helix, β-turn, and β-antiparallel. The logarithmic thin-layer drying mathematical model was the most suitable to simulate the drying process of potato slices under different ultrasonic power values. The above studies showed that ultrasonic pretreatment combined with EHD drying is a promising food drying technology. In future work, a more detailed analysis of ultrasonic pretreatment parameters (such as ultrasonic temperature, ultrasonic time, etc.) and drying mechanism is needed to provide a certain reference for the commercialization of ultrasonic pretreatment.

Data Availability

The data used to support the findings of this study are available from the corresponding author upon request.

Conflicts of Interest

The authors declare that there are no conflicts of interest regarding the publication of this article.

Authors' Contributions

All authors contributed equally to the present study.

Acknowledgments

This research was funded by the National Natural Science Foundations of China (nos. 52067017, 51467015, and 51767020) and Natural Science Foundations of Inner Mongolia Autonomous Region of China (no. 2017MS(LH) 0507).

References

[1] S.-H. Miraei Ashtiani, M. Rafiee, M. M. Morad et al., "Impact of gliding arc plasma pretreatment on drying efficiency and physicochemical properties of grape," *Innovative Food Science and Emerging Technologies*, vol. 63, 2020.

[2] Q. Wang, S. Li, X. Han, Y. Ni, D. Zhao, and J. Hao, "Quality evaluation and drying kinetics of shitake mushrooms dried by hot air, infrared and intermittent microwave-assisted drying methods," *Lebensmittel-Wissenschaft & Technologie*, vol. 107, pp. 236–242, 2019.

[3] Y. Bai, Y. Yang, and Q. Huang, "Combined electrohydrodynamic (EHD) and vacuum freeze drying of sea cucumber," *Drying Technology*, vol. 30, no. 10, pp. 1051–1055, 2012.

[4] L. Shen, Y. Zhu, C. Liu et al., "Modelling of moving drying process and analysis of drying characteristics for germinated brown rice under continuous microwave drying," *Biosystems Engineering*, vol. 195, pp. 64–88, 2020.

[5] H. Xi, Y. Liu, L. Guo, and R. Hu, "Effect of ultrasonic power on drying process and quality properties of far-infrared radiation drying on potato slices," *Food Science and Biotechnology*, vol. 29, no. 1, pp. 93–101, 2020.

[6] A. Singh, V. Orsat, and V. Raghavan, "A comprehensive review on electrohydrodynamic drying and high-voltage electric field in the context of food and bioprocessing," *Drying Technology*, vol. 30, no. 16, pp. 1812–1820, 2012.

[7] T. Anukiruthika, J. A. Moses, and C. Anandharamakrishnan, "Electrohydrodynamic drying of foods: principle, applications, and prospects," *Journal of Food Engineering*, vol. 295, Article ID 110449, 2021.

[8] I. Bashkir, T. Defraeye, T. Kudra, and A. Martynenko, "Electrohydrodynamic drying of plant-based foods and food model systems," *Food Engineering Reviews*, vol. 12, no. 4, pp. 473–497, 2020.

[9] W. Sriariyakul, T. Swasdisevi, S. Devahastin, and S. Soponronnarit, "Drying of aloe vera puree using hot air in combination with far-infrared radiation and high-voltage electric field: drying kinetics, energy consumption and product quality evaluation," *Food and Bioproducts Processing*, vol. 100, pp. 391–400, 2016.

[10] A. Martynenko and W. Zheng, "Electrohydrodynamic drying of apple slices: energy and quality aspects," *Journal of Food Engineering*, vol. 168, pp. 215–222, 2016.

[11] A. Martynenko, I. Bashkir, and T. Kudra, "Electrically enhanced drying of white champignons," *Drying Technology*, vol. 39, no. 2, pp. 234–244, 2019.

[12] T. R. Bajgai and F. Hashinaga, "High electric field drying of Japanese radish," *Drying Technology*, vol. 19, no. 9, pp. 2291–2302, 2001.

[13] T. R. Bajgai and F. Hashinaga, "Drying of spinach with a high electric field," *Drying Technology*, vol. 19, no. 9, pp. 2331–2341, 2001.

[14] A. Esehaghbeygi and M. Basiry, "Electrohydrodynamic (EHD) drying of tomato slices (*Lycopersicon esculentum*)," *Journal of Food Engineering*, vol. 104, no. 4, pp. 628–631, 2011.

[15] X. Cao, M. Zhang, A. S. Mujumdar, Q. Zhong, and Z. Wang, "Effects of ultrasonic pretreatments on quality, energy consumption and sterilization of barley grass in freeze drying," *Ultrasonics Sonochemistry*, vol. 40, pp. 333–340, 2018.

[16] M. Bantle and J. Hanssler, "Ultrasonic convective drying kinetics of clipfish during the initial drying period," *Drying Technology*, vol. 31, no. 11, pp. 1307–1316, 2013.

[17] M. Başlar, M. Kılıçlı, O. S. Toker, O. Sağdıç, and M. Arici, "Ultrasonic vacuum drying technique as a novel process for shortening the drying period for beef and chicken meats," *Innovative Food Science & Emerging Technologies*, vol. 26, pp. 182–190, 2014.

[18] C. I. A. La Fuente and C. C. Tadini, "Ultrasound pre-treatment prior to unripe banana air-drying: effect of the ultrasonic volumetric power on the kinetic parameters," *Journal of Food Science and Technology*, vol. 55, no. 12, pp. 5098–5105, 2018.

[19] J. B. Ni, C. J. Ding, Y. M. Zhang, Z. Q. Song, and W. Q. Xu, "Influence of ultrasonic pretreatment on electrohydrodynamic drying process of goji berry," *Journal of Food Processing and Preservation*, vol. 44, no. 8, 2020.

[20] C. Ding, J. Lu, and Z. Song, "Electrohydrodynamic drying of carrot slices," *PLoS One*, vol. 10, no. 4, Article ID e0124077, 2015.

[21] G. Qiu, Y.-L. Jiang, and Y. Deng, "Drying characteristics, functional properties and in vitro digestion of purple potato

slices dried by different methods," *Journal of Integrative Agriculture*, vol. 18, no. 9, pp. 2162–2172, 2019.

[22] S. Naderinezhad, N. Etesami, A. Poormalek Najafabady, and M. Ghasemi Falavarjani, "Mathematical modeling of drying of potato slices in a forced convective dryer based on important parameters," *Food Sciences and Nutrition*, vol. 4, no. 1, pp. 110–118, 2016.

[23] A. Djebli, S. Hanini, O. Badaoui, B. Haddad, and A. Benhamou, "Modeling and comparative analysis of solar drying behavior of potatoes," *Renewable Energy*, vol. 145, pp. 1494–1506, 2020.

[24] H. Jarahizadeh and S. Taghian Dinani, "Influence of applied time and power of ultrasonic pretreatment on convective drying of potato slices," *Food Science and Biotechnology*, vol. 28, no. 2, pp. 365–376, 2019.

[25] X. F. Wu, M. Zhang, Y. Ye, and D. Yu, "Influence of ultrasonic pretreatments on drying kinetics and quality attributes of sweet potato slices in infrared freeze drying (IRFD)," *Lebensmittel-Wissenschaft und -Technologie- Food Science and Technology*, vol. 131, no. 2, 2020.

[26] A. Puig, I. Perez-Munuera, J. A. Carcel, I. Hernando, and J. V. Garcia-Perez, "Moisture loss kinetics and microstructural changes in eggplant (*Solanum melongena* L.) during conventional and ultrasonically assisted convective drying," *Food and Bioproducts Processing*, vol. 90, no. 4, pp. 624–632, 2012.

[27] X. Duan, M. Zhang, X. Li, and A. S. Mujumdar, "Ultrasonically enhanced osmotic pretreatment of sea cucumber prior to microwave freeze drying," *Drying Technology*, vol. 26, no. 4, pp. 420–426, 2008.

[28] Y.-Y. Zhao, J.-Y. Yi, J.-F. Bi, Q.-Q. Chen, M. Zhou, and B. Zhang, "Improving of texture and rehydration properties by ultrasound pretreatment for infrared-dried shiitake mushroom slices," *Drying Technology*, vol. 37, no. 3, pp. 352–362, 2018.

[29] Y.-X. Bai, G.-J. Yang, Y.-C. Hu, and M. Qu, "Physical and sensory properties of electrohydrodynamic (EHD) dried scallop muscle," *Journal of Aquatic Food Product Technology*, vol. 21, no. 3, pp. 238–247, 2012.

[30] A. Esehaghbeygi, K. Pirnazari, and M. Sadeghi, "Quality assessment of electrohydrodynamic and microwave dehydrated banana slices," *Lebensmittel-Wissenschaft und -Technologie-Food Science and Technology*, vol. 55, no. 2, pp. 565–571, 2014.

[31] M. Yang and C. Ding, "Electrohydrodynamic (EHD) drying of the Chinese wolfberry fruits," *SpringerPlus*, vol. 5, no. 1, p. 909, 2016.

[32] Y. Zhao, W. Wang, B. Zheng, S. Miao, and Y. Tian, "Mathematical modeling and influence of ultrasonic pretreatment on microwave vacuum drying kinetics of lotus (*Nelumbo nucifera* Gaertn.) seeds," *Drying Technology*, vol. 35, no. 5, pp. 553–563, 2016.

[33] Q. Liu, S. Wang, Y. Zheng, Z. Luo, and K. Cen, "Mechanism study of wood lignin pyrolysis by using TG-FTIR analysis," *Journal of Analytical and Applied Pyrolysis*, vol. 82, no. 1, pp. 170–177, 2008.

[34] Y. Chen, C. Zou, M. Mastalerz, S. Hu, C. Gasaway, and X. Tao, "Applications of micro-fourier transform infrared spectroscopy (FTIR) in the geological sciences-A review," *International Journal of Molecular Sciences*, vol. 16, no. 12, pp. 30223–30250, 2015.

[35] S. Bureau, D. Cozzolino, and C. J. Clark, "Contributions of Fourier-transform mid infrared (FT-MIR) spectroscopy to the study of fruit and vegetables: a review," *Postharvest Biology and Technology*, vol. 148, pp. 1–14, 2019.

[36] M. T. Rashid, H. Ma, M. A. Jatoi, M. M. Hashim, A. Wali, and B. Safdar, "Influence of ultrasonic pretreatment with hot air drying on nutritional quality and structural related changes in dried sweet potatoes," *International Journal of Food Engineering*, vol. 15, no. 8, 2019.

[37] J. V. Garcia-Perez, C. Ortuño, A. Puig, J. A. Carcel, and I. Perez-Munuera, "Enhancement of water transport and microstructural changes induced by high-intensity ultrasound application on orange peel drying," *Food and Bioprocess Technology*, vol. 5, no. 6, pp. 2256–2265, 2011.

[38] M. Carbonaro and A. Nucara, "Secondary structure of food proteins by Fourier transform spectroscopy in the mid-infrared region," *Amino Acids*, vol. 38, no. 3, pp. 679–690, 2010.

[39] S. He, J. Shi, E. Walid, H. Zhang, Y. Ma, and S. J. Xue, "Reverse micellar extraction of lectin from black turtle bean (Phaseolus vulgaris): optimisation of extraction conditions by response surface methodology," *Food Chemistry*, vol. 166, pp. 93–100, 2015.

[40] S. Qian, X. Li, H. Wang et al., "Effects of low voltage electrostatic field thawing on the changes in physicochemical properties of myofibrillar proteins of bovine Longissimus dorsi muscle," *Journal of Food Engineering*, vol. 261, pp. 140–149, 2019.